Int. J. Heat Mass Transfer. Vol. 17, pp. 981 990. Pergamon Press 1974. Printed in Great Britain

HEAT TRANSFER IN A ROTARY HEAT EXCHANGER

J. KERN
Department of Chemical Engineering, University of the Witwatersrand, Johannesburg, South Africa

(*Received* 3 *December* 1973)

Abstract—A model for calculating heat transfer in certain types of rotary heat exchangers is presented which allows for a simple way of specifying the main design parameters under given terminal conditions. Energy is exchanged between a granulate being conveyed in an inclined rotating drum and a counter-current gas stream. No flights are considered and radiative exchange is neglected but energy loss through the shell is taken into account. Typical applications are found in the mineral processing industry but the analysis may also be applied to unflighted rotary driers and similar equipment.

NOMENCLATURE

A_n^*, B_n^*, coefficients of the temperature differential equations (3) and (4) [m^{-1}];
A_n, B_n, coefficients of the transformed equations (3a) and (4a);
C_n, D_n,
E, F, coefficients defined in the appendix;
c, specific heat [J/kgK];
h, heat-transfer coefficient [W/m^2K];
k, thermal conductivity [W/mK];
L, total length of heat exchanger [m];
m, mass flow rate [kg/s];
q, heat flux [W];
r, radial coordinate [m];
t, time [s];
T, temperature [°C];
U, overall heat-transfer coefficient from inside shell surface to surroundings [W/m^2K];
y, radial coordinate $r - r_i$ [m];
z, axial coordinate [m].

Greek symbols

α, thermal diffusivity [m^2/s];
β, slope of heat exchanger axis [rad];
Δ, temperature difference of one phase between exchanger inlet and outlet [°C];
ω, rotational frequency [s^{-1}] or [rev/min];
ϕ, filling angle of charge [degrees];
θ, reduced phase temperature $T - T_{z=0}$ [°C];
ζ, reduced axial coordinate z/L.

Subscripts

g, gas phase;
i, related to inside shell surface;
o, related to outside shell surface and surroundings;
s, charge;
w, related to wall material;
sg, between charge and gas;
sw, between charge and wall;
wg, between wall and gas;
wo, between wall and surrounding.

Superscripts

$'$, inlet condition;
$''$, outlet condition.

1. INTRODUCTION

IN A NUMBER of continuous operations granular material has to undergo thermal processing. This is most effectively done in a rotating drum which is slightly inclined in order to ensure a constant flow rate of material. By passing a counter-current gas stream through the apparatus the charge may be dried and heated which is the case for a rotary drier. Other applications are ore roasting or cement formation processes in a rotary kiln where the energy is supplied by a large gas flame burning at the hot end of the kiln. Finally there are also situations where a granulate is merely cooled or heated because further process stages need the material at a certain temperature.

In all these cases specific transfer mechanisms will predominate while others are usually neglected. A rotary drier, e.g. is often designed with flights in order to improve the overall performance. Here one neglects any heat transfer from the shell to the solids and only considers the mechanisms when the particles fall through the gas stream. Extensive analytical studies have been carried out [1, 2], resulting in design equations for flight and drier geometry. They agree fairly well with experimental results [3], but are not applicable to arrangements without flights. In rotary kilns, on the other hand, radiation is the predominating mechanism along the major part of the exchanger. It is therefore not surprising that here the attention is

focussed on a most accurate representation of radiative exchange [4, 5].

However, in both cases the analytical results are not entirely satisfying because they rely strongly on existing data published elsewhere [6, 7]. Important parameters are evaluated from incomplete measurements which impairs the general applicability. When one comes to design a new plant a large amount of uncertainty is left [5]. Certain parameters or constants which are necessary for the calculation are just not available, and the validity of some assumptions in the analysis has been questioned [8]. Own attempts to apply the methods in [4] and [5] to a basically similar arrangement failed so that the results remain doubtful.

The present investigation is a first attempt to obtain results without using specific plant data and therefore should be more generally applicable. However, at this stage the problem is simplified in so far as flights are not taken into account and radiative exchange is assumed to be negligibly small. This limits the application to cases where the temperature difference between charge and wall is not too large and the gas is perfectly transparent. A simple way of solving this problem analytically is developed, which will be modified at a later stage to account for the more complex mechanisms. Unflighted rotary heat exchangers are quite common where the size range of particles is wide because then problems of hold-up and dusting arise [3]. On the other hand the shell may be damaged by coarse material falling down. At high temperatures the inside shell surface normally has to be lined with bricks where then a proper flight design becomes difficult. A typical application, and this motivated the following study, is a cooler following an ore roasting kiln, where abrasive material of extremely wide size range enters at 800–1000°C and has to be cooled down to 200°C or less. Having air as the cooling gas one can neglect radiative exchange and the installation of flights is not suitable for the various reasons pointed out before.

Under these circumstances it turns out that the major part of the energy is transferred indirectly via the shell material. During rotation the inner shell surface is periodically cooled and heated by the gas and charge respectively. In the majority of practical situations the temperature fluctuation will not penetrate to the outside shell surface so that the storage—release mechanism will fully contribute to the energy exchange between gas and charge. It has been shown experimentally [9, 10] that in the preheating zone of a rotary cement kiln this mechanism predominates as well, although flame radiation is taking place at the same time.

Modelling the described indirect transfer mechanism as well as the direct convective exchange and the energy loss through the shell one obtains two coupled linear differential equations for the gas and charge temperatures. These are most conveniently solved by means of Laplace Transforms and one obtains a closed solution for the temperature profiles in the exchanger.

2. FORMULATION OF THE PROBLEM AND GENERAL SOLUTION

In order to illustrate the method most clearly a specific arrangement will be considered throughout the discussion. The decision on which parameters to fix and which to leave variable is arbitrary and may change from one problem to another. Here the exchanger diameters $2r_i$ and $2r_0$ as well as all the physical properties of the gas phase, solid charge and wall material stay constant, because they have a minor influence on the characteristics of the apparatus. The operating conditions are investigated under variable exchanger length, total temperature difference in the charge, rotational frequency of the drum and charge flow rate. In the majority of applications these quantities, some of which are interdependent, will have to be determined towards an economic solution of the specific problem. A constant gas flow rate is assumed, which may look arbitrary, but is true in many practical situations. However, the further analysis will show that a variable gas flow rate could be introduced without further complication.

The general set up is shown in Fig. 1. A hot solid granulate of temperature T_s' enters the inclined rotating drum at $z = L$ and has to be cooled to T_s''. The countercurrent gas stream of temperature T_g' enters at $z = 0$ and is heated to T_g'', where the final temperature will depend on the energy loss through the shell. The outside conditions are characterized by a constant surrounding temperature T_o. With the simplifications introduced earlier the differential energy balance between an arbitrary cross-section z and $z+\mathrm{d}z$ reads as follows (see Fig. 2):

$$\frac{\mathrm{d}q_s}{\mathrm{d}z} = \frac{\mathrm{d}q_{sw}}{\mathrm{d}z} + \frac{\mathrm{d}q_{sg}}{\mathrm{d}z} = m_s c_s \frac{\mathrm{d}T_s}{\mathrm{d}z}. \tag{1}$$

It is assumed that T_s is independent of radial position r, which is equivalent to the "well-mixed" condition in [5]. For a granulate of wide size range and not too low thermal conductivity this is a valid approximation. From Fig. 2 we also find that

$$\frac{\mathrm{d}q_{sw}}{\mathrm{d}z} = \frac{\mathrm{d}q_{wg}}{\mathrm{d}z} + \frac{\mathrm{d}q_{wo}}{\mathrm{d}z},$$

which expresses the steady-state condition of the wall material. Equation (1) thereby becomes

$$m_s c_s \frac{\mathrm{d}T_s}{\mathrm{d}z} = \frac{\mathrm{d}q_{wg}}{\mathrm{d}z} + \frac{\mathrm{d}q_{wo}}{\mathrm{d}z} + \frac{\mathrm{d}q_{sg}}{\mathrm{d}z}. \tag{1a}$$

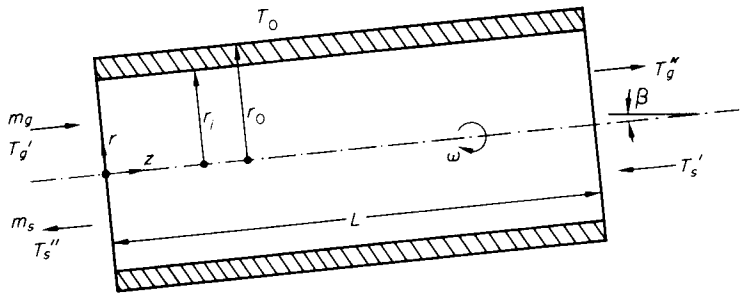

FIG. 1. General set up of a rotary solid-gas heat exchanger.

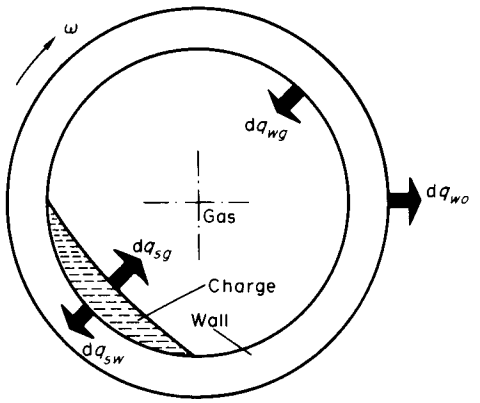

FIG. 2. Differential energy balance for a rotary heat exchanger including energy loss to the surroundings. The charge is cooled by a gas stream.

It follows further that

$$m_g c_g \frac{dT_g}{dz} = \frac{dq_{wg}}{dz} + \frac{dq_{sg}}{dz}. \tag{2}$$

Here the gas temperature is assumed to be independent of r, which is realistic for most practical situations.

If the differential heat flux densities can be expressed as linear functions of the gas and charge temperatures and do not depend on z in any other way then the following equations can be written down:

$$\frac{dT_s}{dz} = A_1^* \times T_s + A_2^* \times T_g + A_3^* \tag{3}$$

and

$$\frac{dT_g}{dz} = B_1^* \times T_s + B_2^* \times T_g + B_3^*. \tag{4}$$

The coefficients A_n^* and B_n^* are functions of the mass flow rates and the rotational frequency as will be shown later. They also contain the physical properties of the materials present, the outside temperature and the exchanger diameters, but these all have been introduced as constants and therefore need not be considered further. As long as the coefficients are independent of z, T_s and T_g the solution to equations (3) and (4) can be obtained in the following way.

The transformation equations

$$\theta_s = T_s - T_s'',$$
$$\theta_g = T_g - T_g'$$

and

$$\zeta = \frac{z}{L}$$

give the two simultaneous differential equations

$$\frac{d\theta_s}{d\zeta} = A_1 \times \theta_s + A_2 \times \theta_g + A_3 \tag{3a}$$

and

$$\frac{d\theta_g}{d\zeta} = B_1 \times \theta_s + B_2 \times \theta_g + B_3 \tag{4a}$$

with the boundary conditions

$$\left.\begin{aligned} &\theta_g(0) = \theta_s(0) = 0 \\ &\theta_s(1) = \Delta_s = T_s' - T_s'' \\ &\text{and} \\ &\theta_g(1) = \Delta_g = T_g'' - T_g'. \end{aligned}\right\} \tag{5}$$

The reason for not introducing the total temperature differences Δ_s and Δ_g into the transformation equations, which would result in dimensionless temperatures, is that we deal with an uninsulated system. T_g'' and T_s' depend on the energy loss through the shell, which can only be specified after having solved the complete problem. The constants A_n and B_n now in addition are functions of the exchanger length and the temperatures at the cold end, T_s'' and T_g'. It is easily seen that, e.g.

$$A_{1,2} = A_{1,2}^* \times L \quad \text{and}$$
$$A_3 = (A_1^* \times T_s'' + A_2^* \times T_g' + A_3^*) \times L.$$

By using the Laplace transformation (see Appendix) equations (3a) and (4a) are solved to give

$$\theta_s(\zeta) = C_1 \times e^{-E\zeta} + C_2 \times e^{-F\zeta} + C_3 \quad (6)$$

and

$$\theta_g(\zeta) = D_1 \times e^{-E\zeta} + D_2 \times e^{-F\zeta} + D_3, \quad (7)$$

where E, F, C_n and D_n are elementary combinations of the original coefficients and are specified in the appendix.

For a given heat exchanger equations (6) and (7) represent the temperature profiles of gas phase and solid charge. Further, as the coefficients contain all the relevant parameters it is easy to study each parameter individually. If, for example, the exchanger length L is to be determined for a certain total temperature difference in the charge Δ_s, where all other parameters are fixed, one sets $\zeta = 1$ in equation (6) and solves for L as a function of $\theta_s(1)$. This will be illustrated further once the coefficients and thus the parameters have been discussed in more detail.

3. MODELLING OF THE HEAT-TRANSFER MECHANISMS

The most important assumption, which leads to the simple solution outlined before, postulates a linear relationship between the differential heat flux densities and the gas and charge temperatures T_g and T_s. The operating conditions for which this is a reasonable approximation have to be analyzed and therefore a more detailed presentation of the modelling process seems to be justified. Analytical expressions for the following three modes of transfer have to be developed:

(a) Indirect transfer from the solids to the gas due to the periodic conduction mechanism in the wall material (dq_{wg});
(b) Conductive/convective transfer through the shell to the outside (dq_{wo});
(c) Direct convective transfer from the solids to the gas (dq_{sg}).

The latter two parts are easily determined if one assumes constant heat-transfer coefficients; they will be discussed later. The major contribution, however, comes from the first transfer process, which is basically similar to the regenerator process. Unfortunately, the large amount of results published in this field cannot be used here because there are some characteristic differences in the analytic treatment. The classical approach [11, 12] always assumes an infinite thermal conductivity of the storage material. This is a good approximation for a regenerator, where the main resistance to heat transfer normally lies in the gas phase and where the period of cycle is of the order of hours. However, the rotary heat exchanger employs a granulate as a heating agent, where then the larger resistance may even lie in the storage material. Further the time available for heating or cooling is of the order of seconds so that a true periodic temperature profile develops in the wall. Therefore also the more recent approaches in the field of regenerator research are not suitable for our purpose; due to the low frequency the periodic problem is always simplified to a transient one [13–15]. In addition, most of the results are obtained in numerical form [15], hence would be difficult to apply to this case.

(a) Storage–release mechanism

With the coordinate system rotating at frequency ω the following equation has to be solved (see Fig. 3):

$$\frac{\partial T_w}{\partial t} = \alpha \frac{\partial^2 T_w}{\partial y^2}. \quad (8)$$

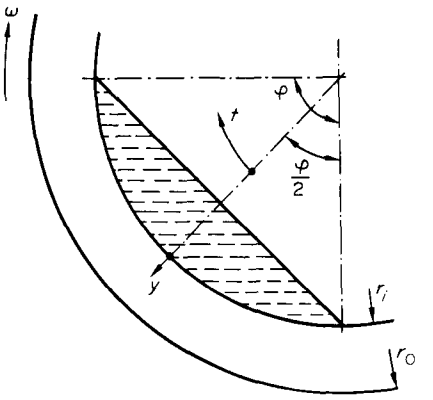

FIG. 3. Model for calculating the indirect energy exchange between charge and gas.

Axial conduction in the z-direction and the curvature of the cylindrical shell are neglected which are commonly used approximations [5]. The boundary conditions are

$$\left.\begin{aligned} h_{sw}(T_s - T_i) &= -k_w \left.\frac{\partial T_w}{\partial y}\right|_{y=0} \quad \text{for} \quad \frac{n}{\omega} \leqslant t \leqslant \frac{n+\dfrac{\phi}{2\pi}}{\omega}, \\ h_{wg}(T_g - T_i) &= -k_w \left.\frac{\partial T_w}{\partial y}\right|_{y=0} \quad \text{for} \quad \frac{n+\dfrac{\phi}{2\pi}}{\omega} \leqslant t \leqslant \frac{n+1}{\omega} \end{aligned}\right\} \quad (9)$$

$$n = 0, 1, 2 \ldots$$

and

$$\left.\frac{\partial T_w}{\partial y}\right|_{y=r_o-r_i,t} = \text{constant}. \quad (10)$$

The condition (10) expresses that the penetration thickness of the oscillation is smaller than the shell thickness, which is valid for most practical situations. Due to the

inhomogeneous boundary condition (9) the problem would have to be solved by some numerical or at least semi-numerical technique [16]. Apart from the fact that this is not the aim of our basic approach there remains the difficulty of determining h_{sw}, the heat-transfer coefficient between the granular bed and the wall. The detailed discussion in [17] shows that especially at elevated temperatures values for h_{sw} are by no means well established. With these arguments in mind the numerical approach is not very promising. Instead, a model is developed which can be treated analytically to give a functional relationship between the variables.

Although we mostly do not know the absolute value of h_{sw}, we can state that it will always be larger than h_{wg} [17]. In the pseudo-steady state the wall temperature T_i then will approach the charge temperature T_s at the end of the heating period. We can draw an approximate temperature profile $T_i(t)$, which depends on the ratio of h_{sw} and h_{wg}. This profile is developed into a Fourier series and serves as the boundary condition for equation (8). As the differential equation is linear one can first solve the problem with the constant in equation (10) being 0, i.e. no heat loss to the outside. Afterwards the latter term is calculated separately. The solution to equation (8) is found in [18]. Differentiating with respect to y, setting $y = 0$ and integrating over either the heating or cooling period, the differential heat flux density $\mathrm{d}q_{wg}$ is obtained.

Two approximate wall temperature distributions are shown in Fig. 4. One realizes immediately that apart from the heat-transfer coefficients the filling angle ϕ and the rotational frequency ω will also affect the performance of the heat exchanger. They both are related to the granulate mass flow rate and the exchanger slope by considering the residence time of the charge. This is commonly expressed by a retention time equation [19]. We see that the problem becomes one of optimizing the rate of energy exchange for a given mass flow rate. Results will be presented at a later stage because here we only want to introduce the general method of rating the heat exchanger.

It has to be pointed out that the assumption of a certain wall temperature profile $T_i(t)$ automatically fixes the average wall temperature which is needed to calculate the energy loss to the surroundings. However, for the immediate purpose the latter can be omitted. We may look at a coarse material where the heat-transfer coefficient h_{sw} is of the same order of magnitude as the wall to gas coefficient h_{wg}. Hence the profile in Fig. 4(a) may be used for the further discussion. The wall temperature as a continuous function of time becomes

$$T_i(t) = \frac{(T_s - T_g)}{4}\frac{32}{3\pi^2}\sum_{n=1}^{\infty}\left[\frac{\sin\dfrac{n\pi}{4}}{n^2}\sin(2n\pi\omega t)\right]. \quad (11)$$

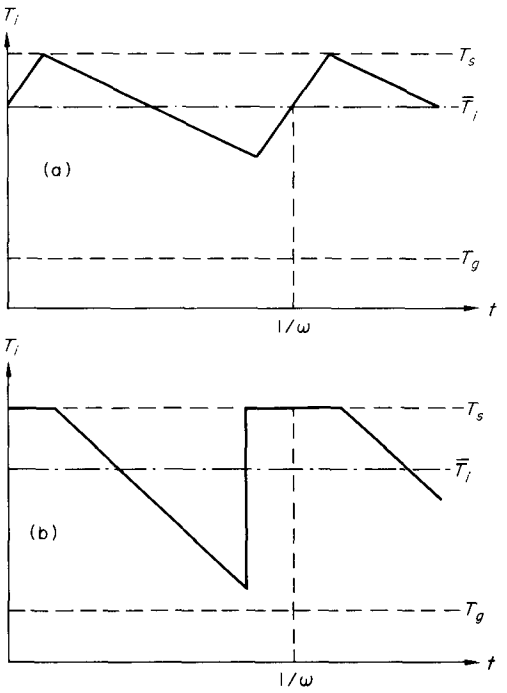

FIG. 4. Approximated wall temperature distributions on the inside shell surface. (a) $\phi = \pi/2$, $h_{sw}/h_{wg} = 3$; (b) same h_{wg}, but $h_{sw}/h_{wg} = \infty$, $\phi = 2/3\pi$ and half the rotational frequency.

The solution to equation (8) subject to the boundary condition (11) is

$$T_w(y,t) = \frac{32(T_s - T_g)}{12\pi^2}\sum_{n=1}^{\infty}\left[\frac{\sin\dfrac{n\pi}{4}}{n^2}e^{-y\sqrt{(n\pi\omega/\alpha)}} \times \sin\left[2n\pi\omega t - y\sqrt{(n\pi\omega/\alpha)}\right]\right]. \quad (12)$$

Differentiating equation (12) with respect to y and setting $y = 0$, we get

$$-k_w\left.\frac{\partial T_w}{\partial y}\right|_{y=0} = \frac{32(T_s - T_g)k_w}{12\pi^2}\sqrt{(\pi\omega/\alpha)} \sum_{n=1}^{\infty}\left[\frac{\sin\dfrac{n\pi}{4}}{n\sqrt{n}}(\sin 2n\pi\omega t + \cos 2n\pi\omega t)\right]. \quad (13)$$

Integration over the cooling period $1/8\omega \leqslant t \leqslant 7/8\omega$ (see Fig. 4a) yields after some rearrangement

$$q_{wg} = \frac{32(T_s - T_g)k_w}{12\pi^2}\sqrt{(\pi\omega/\alpha)} \times \sum_{n=1}^{\infty}\left[\frac{(-1)^n\left(\cos\dfrac{n\pi}{2} - (-1)^n\right)}{n^2\sqrt{n}}\right]. \quad (14)$$

The series converges rapidly, the change between

$$\sum^{9} \quad \text{and} \quad \sum^{10}$$

is less than 0·3 per cent

$$\sum_{n=1}^{\infty} \simeq 1{\cdot}5(\pm 0{\cdot}5 \text{ per cent}).$$

Equation (14) has to be multiplied by $2\pi r_i\omega$ to give the differential heat flux density per m of exchanger length as defined earlier

$$\frac{\mathrm{d}q_{wg}}{\mathrm{d}z} = 0{\cdot}72\, r_i k_w \sqrt{(\omega/\alpha)}(T_s - T_g). \tag{15}$$

Thus the linear relationship between $\mathrm{d}q$ and the gas and charge temperatures is established in an analytical form and all the relevant parameters are represented as well. The constant 0·72 will change when a different profile $T_i(t)$ is assumed but the characteristics of equation (15) will remain the same.

(b) Conductive–convective transfer to the outside

The steady-state energy loss to the surroundings can be written as

$$\frac{\mathrm{d}q_{wo}}{\mathrm{d}z} = U_i \times 2\pi r_i(\bar{T}_i - T_o). \tag{16}$$

Here $\bar{T}_i$ is the time averaged wall temperature on the inside shell surface, which is a given linear function of T_s and T_g. From Fig. 4(a) we have

$$\bar{T}_i = \frac{3T_s + T_g}{4}$$

as an approximate average. T_o normally is constant. U_i is the overall heat-transfer coefficient related to the inside shell surface and for composite walls is a function of the shell dimensions, shell properties and the outside heat-transfer coefficient h_o. The calculation of h_o from existing correlations [20] will already need the outside wall temperature, which is not known at this stage and varies with z. As this would yield a nonlinear relationship between $\mathrm{d}q_{wo}$ and T_s and T_g a constant value of h_o has to be estimated from the values at $z = 0$ and $z = L$. However, the loss in accuracy normally is small; if the variation of h_o with z is extremely large, the exchanger may have to be divided into subsections.

(c) Direct convective transfer from the charge to the gas

This often makes only a minor contribution to the total exchange rate so that the assumption of a constant heat-transfer coefficient h_{sg} is not critical. With the gas-charge interface being a function of the filling angle ϕ the differential heat flux density becomes

$$\frac{\mathrm{d}q_{sg}}{\mathrm{d}z} = h_{sg} 2r_i \sin\left(\frac{\phi}{2}\right)(T_s - T_g), \tag{17}$$

where values for h_{sg} can be taken from well-known correlations [20].

Equations (15)–(17) all represent linear relationships between heat flux density and charge and gas temperatures so that the developed method for solving equations (1a) and (2) can be applied. The coefficients C_n, D_n, E and F are obtained directly from the physical relations set up in this section once the materials involved are known and some basic process data have been specified.

4. RESULTS AND DISCUSSION

As mentioned before the further discussion will be concentrated on the main operating parameters which are the charge flow rate, the rotational frequency of the cylinder and the total charge temperature difference. The dependent variable is the length of the exchanger; its diameters as well as all the materials are fixed. Further we assume that the filling angle ϕ and the wall temperature distribution according to Fig. 4(a) remain unchanged. This, of course is a severe simplification. It is clear that with increasing frequency and decreasing charge flow rate the filling angle decreases (see also [3]) and that for constant heat-transfer coefficients h_{sw} and h_{wg} the wall temperature profile must change with ω. However, the detailed analysis will be presented at a later stage so that at present we may specify a constant ratio h_{sw}/h_{wg}. Further we assume that the varying charge flow rate is coupled to a varying exchanger slope in such a way that the filling angle stays constant. The necessary data, which have been taken from an operating heat exchanger, are collected in Table 1.

In various situations it is important to know how the temperatures change along the heat exchanger. The lining mostly acts as a thermal protection of the carrying shell, hence is only necessary above a certain charge temperature. A typical temperature distribution is shown in Fig. 5. Under the specified conditions one evaluates the coefficients from equations (A-5) and (A-8–A-13) to obtain the following relations:

$$T_s[^\circ\mathrm{C}] = 273\mathrm{e}^{0{\cdot}02z} - 101\mathrm{e}^{-0{\cdot}06z} + 28$$

and

$$T_g[^\circ\mathrm{C}] = 233\mathrm{e}^{0{\cdot}02z} - 230\mathrm{e}^{-0{\cdot}06z} + 23.$$

For a required cooling Δ_s one finds the necessary exchanger length L from equation (6) by setting $\zeta = 1$ and solving for L. The temperature profiles show a marked inflexion point which is due to the following fact: the energy loss to the surroundings is proportional

Table 1

Solid charge	Gas phase	Heat-transfer coefficients
$c_s = 0{\cdot}2$ Wh/kgK	$c_g = 0{\cdot}29$ Wh/kgK	$h_o = 5$ W/m^{2}K
$\phi = \frac{\pi}{2}$	$m_g = 10^4$ kg/h	$h_{sg} = 1{\cdot}5$ W/m^{2}K
$T_s'' = 200$°C	$T_g' = T_o = 30$°C	$\frac{h_{sw}}{h_{wg}} = 3$
Heat exchanger		
$r_i = 1{\cdot}82$ m; $k_w = 1{\cdot}0$ W/mK; $\alpha_w = 4{\cdot}3 \times 10^{-7}$ m^2/s	$r_o = 2{\cdot}00$ m; $k_{st} = 20$ W/mK;	$\Delta r_w = 0{\cdot}15$ m (lining) $\Delta r_{st} = 0{\cdot}03$ m (steel shell)

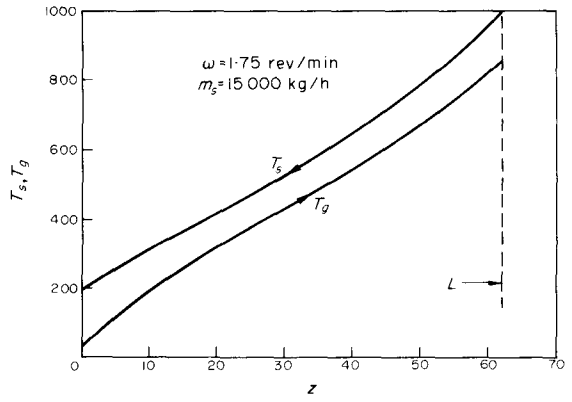

FIG. 5. Typical temperature profiles for charge (T_s) and gas (T_g) in a rotary heat exchanger.

to the charge and gas temperatures [see equation (16)], therefore dq_{wo} will increase from the cold to the hot end of the exchanger. At low temperatures this effect is small so that the energy exchange between charge and gas will decrease with z, which gives convex profiles. However, when an essential fraction of the energy is lost through the shell then the gas temperature profile will more or less follow the charge profile so that both become concave. The actual point of inflexion will largely depend on the value of U_i, the overall heat-transfer coefficient defined earlier.

However, in most cases one wants to know how long the heat exchanger has to be to achieve a certain cooling Δ_s and how this required length varies with charge flow rate and rotational frequency. For that purpose Figs. 6 and 7 have been put up. It is seen that

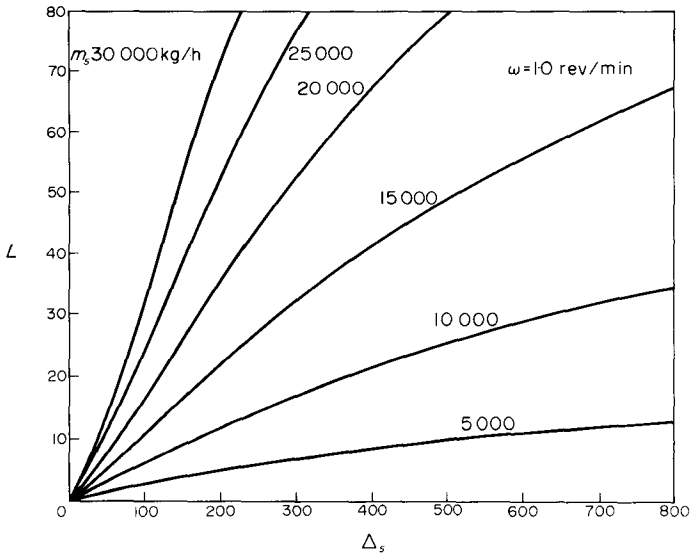

FIG. 6. Required heat exchange length L for variable charge cooling Δ_s and mass flow rate m_s.

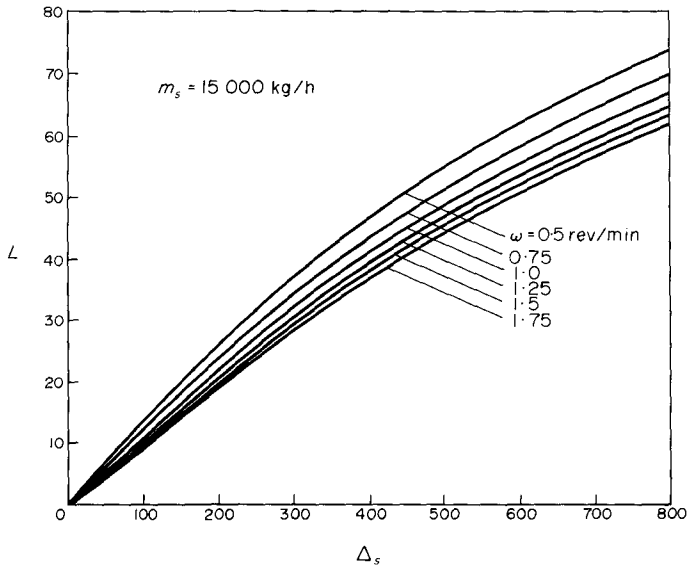

FIG. 7. Required heat exchanger length L for variable charge cooling Δ_s and rotational frequency ω.

the charge flow rate has a very strong influence on L; therefore it may easily happen that a cooler is thermally overloaded. This can only partially be compensated by an increased rotational frequency as is shown in Fig. 7. The comparatively moderate influence of ω on the required length is a result of the unfavourable wall temperature distribution chosen in Fig. 4(a). The storage-release mechanism in that case provides only up to half the energy loss of the solids, whereas in other cases represented by Fig. 4(b) up to 75 per cent of the total energy loss is due to the periodic exchange. Apart from that the chosen charge flow rate in Fig. 7 seems to be already so high that the energy exchange is controlled by the gas flow rate. This is indicated by the inflexion point in the corresponding curve in Fig. 6.

The outlined behaviour is illustrated further in Fig. 8. The absolute change in exchanger length for variable rotational frequency is larger at higher charge flow rates.

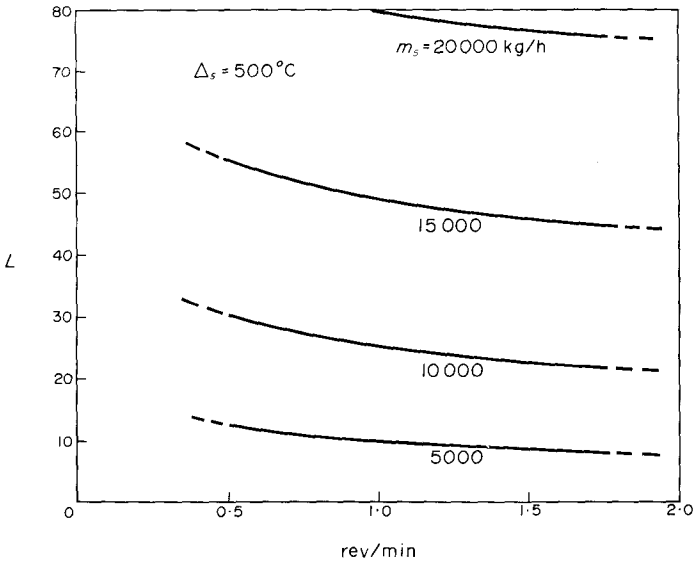

FIG. 8. Variation of required heat exchanger length L with rotational frequency ω and charge flow rate m_s.

However, the relative change is essentially bigger for the smaller flow rates in comparison with the larger ones. This applies even more to smaller coolings Δ_s, where the energy loss to the surroundings has only a minor influence. What can now only be seen as a tendency will come out more clearly once the interdependence of ω, m_s and various other parameters has been developed more strictly. Then the frequency can be varied over a wider range and the described relationships will be more marked.

5. CONCLUSION

The performance of rotary solid-gas heat exchangers has been studied under variable operating conditions. After modelling the different heat-transfer mechanisms a simple method is devised, which allows one to calculate the temperature distributions of gas and solid charge along the exchanger. Once these temperature profiles are known in an analytical form the influence of various operating parameters like charge flow rate or rotational frequency of the exchanger can be investigated. It turns out that under certain conditions the apparatus may become thermally overloaded and a required charge cooling is only achieved with an uneconomically long exchanger. The rate of energy exchanged indirectly via the shell material depends on the assumed wall temperature distribution $T_i(t)$. It may require some physical insight to establish this distribution, but in turn one obtains a simple solution to the problem.

It has to be pointed out that this study is only a first attempt to get analytical results for a basically complex problem. Various parameters like gas flow rate, exchanger slope and residence time of the charge remained undiscussed and radiative energy exchange as well as flight installation were not considered here. The aim was to illustrate the approach and sophistications will be introduced at a later stage.

Acknowledgement—The author wishes to thank the staff of Ucar Ltd., Pretoria, for valuable practical suggestions and for making available certain data.

REFERENCES

1. S. J. Porter, The design of rotary driers and coolers, *Trans. Inst. Chem. Engrs* **41**, 272–280 (1963).
2. G. A. Turner, The thermal history of a granule in a rotary cooler, *Can. J. Chem. Engng* **44**, 13–16 (1966).
3. S. J. Friedman and W. R. Marshall, Studies in rotary drying, Pts. I and II, *Chem. Engng Progr.* **45**, 482–493 and 573–588 (1949).
4. A. Sass, Simulation of the heat transfer phenomena in a rotary kiln, *I/EC Process Des. Dev.* **6**, 532–535 (1967).
5. M. Imber and V. Paschkis, A new theory for a rotary-kiln heat exchanger, *Int. J. Heat Mass Transfer* **5**, 623–638 (1962).
6. W. Gilbert, Investigations on a slurry drier or calcinator—II, *Cement & Cement Manuf.* **9**, 139–154 (1936).
7. H. Gygi, The thermal efficiency of a rotary cement kiln—IV (cont.). Heat transfer, *Cement & Lime Manuf.* **11**, 143–153 (1938).
8. V. A. Kaiser and J. W. Lane, Correspondence on [4], *I/EC Process Des. Dev.* **7**, 318–319 (1968).
9. H. Gygi, The thermal efficiency of a rotary cement kiln—IV (cont.). Heat transfer, *Cement & Lime Manuf.* **11**, 133–141 (1938).
10. H. Gygi, The thermal efficiency of a rotary cement kiln –IV. Heat transfer, *Cement & Lime Manuf.* **11**, 79–84 (1938).
11. H. Hausen, Näherungsverfahren zur Berechnung des Wärmeaustausches in Regeneratoren, *Z. Angew. Math. Mech.* **11**, 105–114 (1931).
12. G. Ackermann, Die Theorie der Wärmeaustauscher mit Wärmespeicherung, *Z. Angew. Math. Mech.* **11**, 192–205 (1931).
13. P. Razelos and A. Lazaridis, A lumped heat-transfer coefficient for periodically heated hollow cylinders, *Int. J. Heat Mass Transfer* **10**, 1373–1387 (1967).
14. D. Handley and P. J. Heggs, The effect of thermal conductivity of the packing material on transient heat transfer in a fixed bed, *Int. J. Heat Mass Transfer* **12**, 549–570 (1969).
15. F. W. Larsen, Rapid calculation of temperature in a regenerative heat exchanger having arbitrary initial solid and entering fluid temperatures, *Int. J. Heat Mass Transfer* **10**, 149–168 (1967).
16. J. R. Reed and G. Mullineux, Quasi-steady state solution of periodically varying phenomena, *Int. J. Heat Mass Transfer* **16**, 2007–2012 (1973).
17. S. S. Zabrodsky, Compound heat exchange between a high temperature gasfluidized bed and a solid surface, *Int. J. Heat Mass Transfer* **16**, 241–248 (1973).
18. H. S. Carslaw and J. C. Jaeger, *Conduction of Heat in Solids*, 2nd Edn. Clarendon Press, Oxford (1959).
19. J. D. Sullivan, G. C. Maier and O. C. Ralston, U.S. Bur. Mines Tech. Paper 384 (1927
20. A. J. Chapman, *Heat Transfer*, 2nd Edn. Macmillan, New York (1969).

APPENDIX

With the boundary condition (5) the Laplace transformation of equations (3a) and (4a) gives the two algebraic equations

$$s \times \bar{\theta}_s = A_1 \times \bar{\theta}_s + A_2 \times \bar{\theta}_g + A_3/s \qquad \text{(A-1)}$$

and

$$s \times \bar{\theta}_g = B_1 \times \bar{\theta}_s + B_2 \times \bar{\theta}_g + B_3/s. \qquad \text{(A-2)}$$

The bar indicates the Laplace domain, the dependent variable now is s. After rearrangement we obtain

$$\bar{\theta}_s = \frac{A_2 \times B_3 - B_2 \times A_3}{s[(s-A_1)(s-B_2) - A_2 \times B_1]} + \frac{A_3}{(s-A_1)(s-B_2) - A_2 \times B_1} \qquad \text{(A-3)}$$

and

$$\bar{\theta}_g = \frac{B_1 \times A_3 - A_1 \times B_3}{s[(s-A_1)(s-B_2) - A_2 \times B_1]} + \frac{B_3}{(s-A_1)(s-B_2) - A_2 \times B_1}. \qquad \text{(A-4)}$$

For inversion the expression in square brackets has to be converted as follows:

$$[(s-A_1)(s-B_2)-A_2\times B_1]=(s+E)(s+F)$$

where

$$E,F=-\left(\frac{A_1+B_2}{2}\pm\sqrt{\left[\left(\frac{A_1+B_2}{2}\right)^2+A_2\times B_1-A_1\times B_2\right]}\right). \quad \text{(A-5)}$$

Then

$$\bar{\theta}_s=\frac{A_2\times B_3-A_3\times B_2}{s(s+E)(s+F)}+\frac{A_3}{(s+E)(s+F)} \quad \text{(A-6)}$$

and

$$\bar{\theta}_g=\frac{A_3\times B_1-A_1\times B_3}{s(s+E)(s+F)}+\frac{B_3}{(s+E)(s+F)}. \quad \text{(A-7)}$$

After elementary inversion and rearrangement one gets equations (6) and (7), where the coefficients are

$$C_1=\frac{A_2\times B_3-B_2\times A_3-A_3\times E}{E(E-F)}, \quad \text{(A-8)}$$

$$C_2=\frac{A_3\times F-A_2\times B_3+B_2\times A_3}{F(E-F)}, \quad \text{(A-9)}$$

$$C_3=\frac{A_2\times B_3-B_2\times A_3}{E\times F}, \quad \text{(A-10)}$$

$$D_1=\frac{A_3\times B_1-A_1\times B_3-B_3\times E}{E(E-F)}, \quad \text{(A-11)}$$

$$D_2=\frac{B_3\times F-A_3\times B_1+A_1\times B_3}{F(E-F)}, \quad \text{(A-12)}$$

$$D_3=\frac{A_3\times B_1-A_1\times B_3}{E\times F}. \quad \text{(A-13)}$$

Equations (A-5) and (A-8)–(A-13) thus are simple combinations of the original coefficients and once these are specified the temperature profiles can be calculated from equations (6) and (7).

TRANSFERT DE CHALEUR DANS UN ECHANGEUR ROTATIF

Résumé—On présente un modèle pour calculer le transfert thermique dans certains types d'échangeurs rotatifs. Il donne de façon simple les paramètres essentiels pour des conditions terminales données. L'énergie est échangée entre un milieu granulaire convoyé dans un tambour tournant incliné et un écoulement gazeux à contre-courant. On néglige le vol de particules et l'échange par rayonnement, mais on tient compte des pertes de chaleur à travers la paroi. On trouve des applications typiques dans l'industrie du traitement des minéraux, mais l'analyse peut être appliquée aux séchoirs rotatifs et aux équipements similaires.

WÄRMEÜBERTRAGUNG IN ROTIERENDEN WÄRMEÜBERTRAGERN

Zusammenfassung—Für verschiedene Arten rotierender Wärmeübertrager wird ein mathematisches Modell zur Berechnung des Wärmeüberganges angegeben. Damit ist es auf einfache Weise möglich, die maßgeblichen Parameter zu bestimmen. Wärme wird bei Gegenstromführung von Granulat und Gas ausgetauscht. Das Granulat wird hierbei durch eine geneigt angeordnete, rotierende Trommel gefördert. Es wird geordnete Bewegung des Granulats angenommen. Der Wärmeaustausch durch Strahlung wird vernachlässigt, der Energieverlust in der Trommel wird jedoch berücksichtigt. Typische Anwendungsfälle sind in der mineralien-verarbeitenden Industrie anzutreffen. Das Berechnungsmodell kann jedoch auch auf Trommeltrockner und ähnliche Apparate übertragen werden.

ТЕПЛООБМЕН ВО ВРАЩАЮЩЕМСЯ ТЕПЛООБМЕННИКЕ

Аннотация — Приводится расчётная модель теплообмена в некоторых типах ротационных теплообменников, дающая простой способ определения основных параметров конструкции при заданных граничных условиях. Перенос тепла происходит между перебрасываемыми в наклонном вращающемся барабане гранулами и встречным потоком газа. При этом не рассматривается случай наличия ребер на внутренней поверхности теплообменника, пренебрегается лучистым теплообменном, но учитываются тепловые потери через оболочку. Такие теплообменники широко применяются в горнодобывающей промышленности. Результаты анализа могут быть также использованы для расчёта неоребренных барабанных сушилок и аналогичного оборудования.